OFFLINE ARTERIAL SIGNAL TIMING OPTIMIZATION BASED ON VIRTUAL PHASE LINK MODEL - A REAL-WORLD CASE STUDY

Qichao Wang, Ph.D. (Corresponding Author)
National Renewable Energy Laboratory
15013 Denver West Parkway, Golden, CO, 80401.
Email: Qichao.Wang@nrel.gov

Joseph Severino
National Renewable Energy Laboratory
15013 Denver West Parkway, Golden, CO, 80401.
Email: Joseph.Severino@nrel.gov

Juliette Ugirumurera, Ph.D.
National Renewable Energy Laboratory
15013 Denver West Parkway, Golden, CO, 80401.
Email: jugirumu@nrel.gov

Wesley Jones, Ph.D.
National Renewable Energy Laboratory
15013 Denver West Parkway, Golden, CO, 80401.
Email: Wesley.Jones@nrel.gov

Jibonananda Sanyal, Ph.D.
Oak Ridge National Laboratory
Oak Ridge, TN 37831
Email: sanyalj@ornl.gov

Word Count: 4046 words + 0 table(s) $\times$ 250 = 4046 words

Submission Date: August 1, 2020

ABSTRACT

Conventional signal timing for arterial usually takes bottom-up approaches. Engineers optimize each individual intersection first and then coordinate them by adjusting the offsets. This work is based on the Virtual Phase-Link (VPL) model, a street traffic model designed for online traffic model predictive control, to obtain a top-down offline arterial signal timing. We Studied the Shallowford Rd. in Chattanooga, TN and found that the inconsistency in intersection capacities along the arterial could lead to some intersections becoming bottlenecks. Signal timing is a significant factor that affect the intersection capacities. We realized that the VPL-based model can guarantee the consistency in intersections along an arterial. We therefore adopted the VPL-based model and developed an offline signal timing optimization approach. The proposed timing derived from the VPL-based offline signal timing optimization showed very good results in simulation. The Chattanooga Department of Transportation adopted the optimized timing obtained from the proposed approach and gave positive feedbacks to the research team. We also collected field experiment data, which demonstrated overall energy reductions and speed improvements on some sections of the Shallowford Rd. arterial. We will continue the experiment when the COVID-19 pandemic impact subsides to have a more robust quantitative evaluation.

Keywords: VPL model, Offline Signal Timing, Arterial

INTRODUCTION

An Arterial with closely spaced intersections are sensitive to the fluctuation in traffic volumes. Phase failures at one intersection could cause queue spilling back which leads to the failure in control in the upper stream intersection. In this kind of arterials, the standard bottom-up signal timing approach (considering each intersection individually and then adjusting the control parameters to coordinate) could easily cause the failure in control along the arterial. The observed traffic flow within the arterial are usually impacted by the surrounding controls. The traffic volume counts from advanced system detectors around the boundary of the arterial are used for each individual intersection's timing. While the traffic volumes from the network boundary impact the whole arterial, this information are usually not fully utilized for the signal timing of the whole arterial. There is a need to consider an area as a whole and to take a top-down signal timing approach for arterial or grid network where intersections are closely spaced.

One of the major research efforts in arterial signal control focuses on fine-tuning the signal offsets (*1, 2*). Although tuning offsets has the most potential to improve arterial traffic signal control performance, arterials with closely spaced intersections are most vulnerable to unbalanced splits setting.

Wang and Abbas showed that coordinating green splits among arterial intersections can also have significant impacts on the arterial performance (*3, 4*). They proposed a real-time splits optimization algorithm through Model Predictive Control (MPC). This algorithm requires real-time knowledge of traffic space distribution on the road network. The set of signal timings along arterial can be obtained to optimize the whole arterial via simulation-based optimization (*5, 6*). However, this approach becomes computationally expensive as the studied area becomes larger.

System-level controls of an arterial can be addressed by traffic responsive control or adaptive traffic control (*3, 7–9*). However, many regions in the world still lack real-time automatic traffic state detection. There is a need to have an approach to help design arterial signal timing offline and still provide good reliability in control.

One of the focus of recent offline signal timing research is to address the uncertainties in traffic demand. Yin (*10*) presented scenario-based mean-variance optimization, scenario-based conditional value-at-risk minimization, and min-max optimization for traffic signal timing using the Highway Capacity Manual (HCM) delay equation (*11*) for isolated fixed-time signalized intersections. Liu et al. applied distributionally robust optimization to address the uncertainties in turning ratios (*12*). Both research addressed the uncertainty by optimizing the signal timings for a set of possible scenarios in the real-world.

This work is built on the Virtual Phase-Link (VPL) model designed for the MPC algorithm proposed by Wang and Abbas (*3*). We utilized the VPL model to obtain offline arterial signal timings for the studied intersections in a top-down manner. We focused on the split allocations for arterials with closely spaced intersections during peak hours. We addressed the uncertainties in the real-world by optimizing a constant control strategy for the VPL model for a large number of control cycles. We were not controlling the signal timing with real-time traffic state, and the traffic state will not be constant in the field. Therefore, we optimized the signal timing for a large number of control cycles since in each cycle, there will be a different traffic state.

This work is part of the Regional Mobility project, which seeks to use situational awareness and traffic control to reduce traffic energy consumption (*13*). This paper focuses on a field experiment that we conducted in Chattanooga, TN in late February, 2020. We conducted the following procedures in this experiment: 1) selected the intersections to be controlled, 2) identified the main

traffic issue along the arterial, 3) found a cause of bottleneck in arterial signal control, 4) modified and applied the VPL-based signal control to obtain an optimal signal timing that avoided the bottleneck, 5) tested the new timing in Vissim simulation against the existing timing, 6) proposed the new timings to Chattanooga Department of Transportation (DOT) and had the timing implemented. From the simulation results, we found that the optimized timing can move the traffic under very congested condition and was able to improve throughput, reduce delay and fuel consumption along the arterial. We received positive feedback from the Chattanooga DOT for the field experiment.

METHODOLOGY

Study Site

In this project, we chose Shallowford Rd. in Chattanooga, TN, shown in Figure 1, as the study site. We further selected four intersections to optimize the timing, i.e., Shallowford Rd. and Amin Dr. (referred as intersection A), Shallowford Rd. and SB Ramp (referred as intersection B), Shallowford Rd. and NB Ramp (referred as intersection C), and Shallowford Rd. and Napier Rd. (referred as intersection D). We studied the afternoon peak time as specified the controllers under the current settings, which is 4 pm to 7:30 pm, for study. Figure 1 shows the four intersections (circled in red) that were studied in this work. We selected to study these four intersections along Shallowford Rd. arterial for the following reasons:

- These intersections were instrumented with video detection cameras which can provide traffic flow, turning ratio, real-time video feed, and historical signal timing statistics.
- These four intersections covered the most congested area near the mall (as shown in Figure 1) during afternoon peak time.
- These intersections were closely spaced which cause queue spill back easily.

It should be noted that intersection B and intersection C at the diamond interchange ramps were controlled by separate controllers. Therefore, we did not consider the three-phase or Texas Transportation Institute (TTI) four-phase scheme (*14*). The proposed signal timing approach can be applied to a general arterial without the need to include an interchange.

By interviewing local travelers and Chattanooga DOT, we found that the eastbound was the most congested movement and the most congested location was on the bridge (from intersection B to intersection C). The main issue in the study site is queue spilling back to the upstream intersection and causing failure in signal control in the upstream intersection. The congestion on the eastbound bridge (between intersection B and intersection C) was caused by the queue spilled back at intersection D. Even when there was long green time for the eastbound traffic at intersection C, the vehicles could not fully use the green time. This was because the queue from intersection D already reached intersection C and prevented vehicles from entering intersection C.

Arterial Bottleneck from Capacity Inconsistency

When queue spills back to an upper stream intersection, the upper stream intersection's control will fail. An optimally controlled arterial should at least prevent queue spilling back to an upper stream intersection. The road links have space storage capacity to hold vehicles when traffic become congested. An arterial with closely spaced intersections only have limited storage capacity for each road link to hold the vehicles. In this case, queue spilling back becomes a critical phenomenon to prevent from. From a queuing system's point of view, a necessary condition for preventing queue spilling back is to have the system's average service rate to be greater than the average arrival rate.

The service rate of an intersection is its capacity. The signalized intersection's capacity of

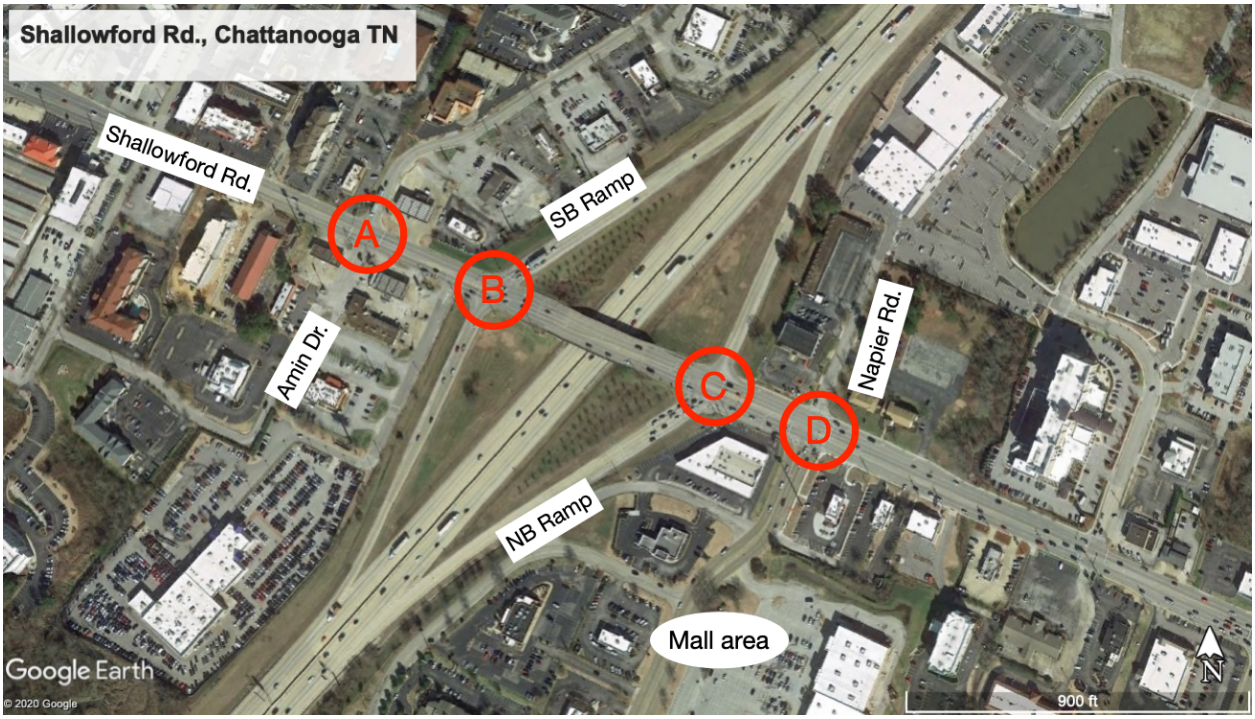

FIGURE 1 The study site.

a certain movement, m, can be calculated with Equation 1.

$$c_{i,m} = s_{i,m} \times \frac{g_{i,m}}{C_i} \tag{1}$$

Where:

$c_{i,m}$: capacity of movement m at intersection i;

$s_{i,m}$: saturation flow rate of movement m at intersection i;

$g_{i,m}$: green time of the phase that allows movement m at intersection i; and

C_i: cycle length of the controller at intersection i.

During peak hours, the traffic tends to fully use the green times at or near the saturation flow rate. The incoming flow was released from the upper stream intersection. The maximum incoming flow rate $\lambda^+_{i,p}$ of intersection i movement p can be calculated with Equation 2.

$$\lambda^+_{i,p} = \sum_{q \in Q_{i,p}} c_{i-1,q} = \sum_{q \in Q_{i,p}} s_{i-1,q} \times \frac{g_{i-1,q}}{C_{i-1}} \tag{2}$$

Where:

$Q_{i,p}$: the set of movements that flow into movement p at intersection i.

Similar to highway bottlenecks, the inconsistency in signalized intersections' capacities along the arterial also causes bottlenecks.

Figure 2 shows the NEMA phase diagram of Shallowford and NB ramp intersection (as noted in 1). The numbers in circles indicate each phase's movement. Phase 1 was associated with phase 6 and was not marked in the map. Phase 4 included the northbound left turn and right turn movement. From the NEMA diagram, we can see that the flow into the eastbound movement of Shallowford Rd. and Napier Rd. are almost continuous in the control cycle (except for the lost time of phase 6 and phase 4). During peak hours, the traffic flow into link A are alternating between

the saturation flow from the through movement of phase 6 and the saturation flow from the right turn of phase 4. If we want to match the inflow of intersection D eastbound movement, applying Equation 1 and 2, we found that the green time for the eastbound through movement at intersection D should at least take 70% of the cycle length. However, the historical report showed that the green time allocation was never exceeding 50% of the cycle length.

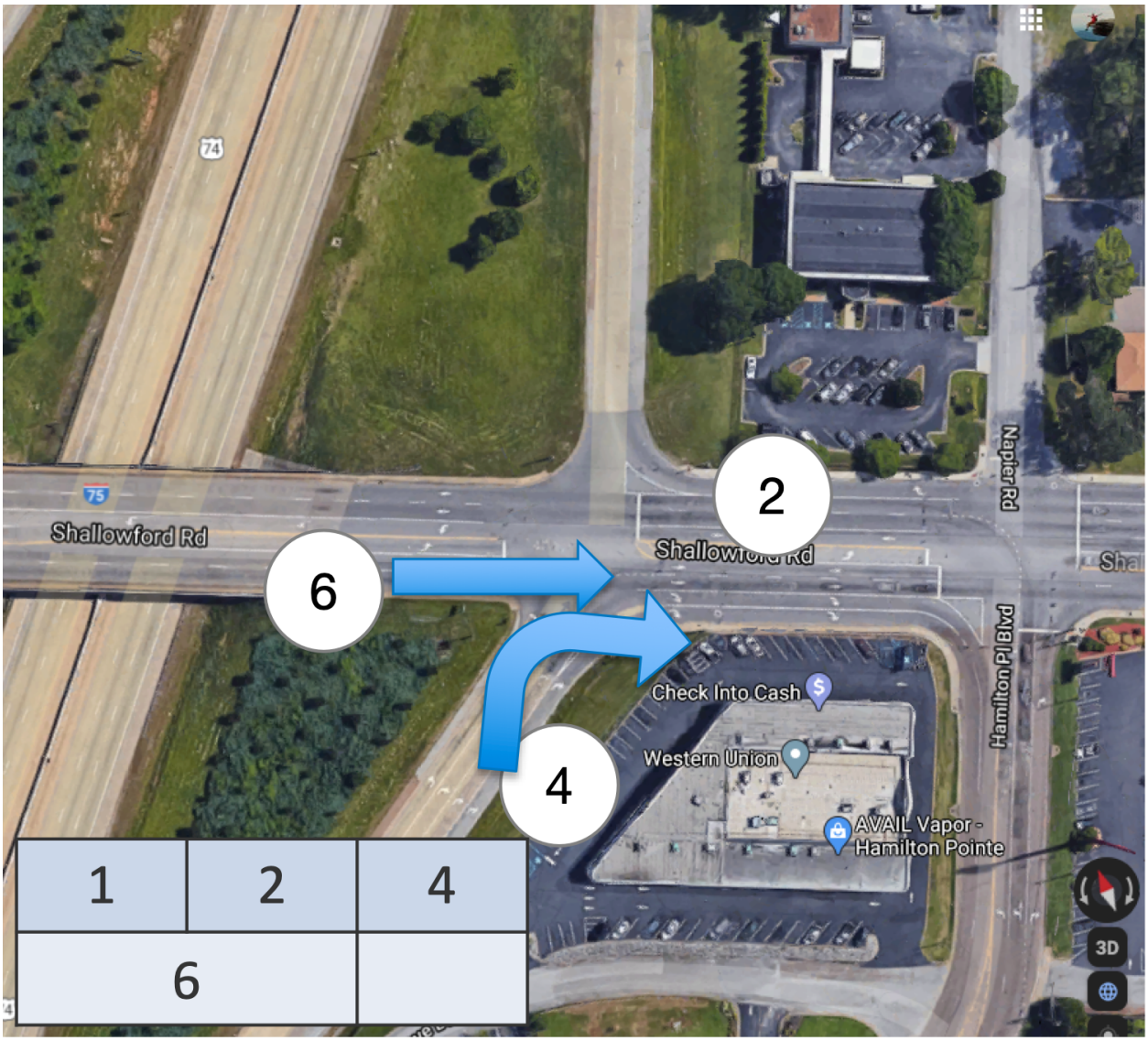

FIGURE 2 Shallowford Rd. and NB Ramp intersection and its NEMA diagram

VPL Model and Modified VPL Model to Address Channelized Right-turn Lanes

We realized that the street traffic signal Model Predictive Control (MPC) based on the (Virtual Phase-Link) VPL model (*3*) implied the consistency in the arterial capacities across intersections. The VPL model in our previous work was designed for a general case. We need to modify the VPL model to address the uncontrolled channelized right turn lanes (e.g., westbound right turn into the ramp at the NB intersection).

To make this paper self contained, we summarize the original VPL model here. The vehicles on a road link could be served by multiple phases. We define a VPL, (i,p), as a virtual link that only holds vehicles that will be served by one phase, p, at a intersection, i. The VPL model describe a dynamic system of the street traffic. The road network is described a set of VPL in the VPL model. The topology of the network is described by the set of upstream VPLs, $V_{(i,p)}$, of a VPL, (i,p). The impact of number of lanes are captured in the saturation flow rate, $s_{i,p}$, for phase p at intersection i. The states of the system are the numbers of vehicles, $X_{(i,p)}(\cdot)$, in each VPL, (i,p). The number of vehicles in a VPL should be less than the space capacity of the VPL, i.e., $X_{(i,p)}(\cdot) \in [0, c_{(i,p)}]$. The control of the system is the allocated green time of phase p, $u_{i,p}(\cdot)$, and the fully used green time equivalent of VPL (i,p), $G_{(i,p)}(\cdot)$. The fully used green time equivalent and any time step k should be none negative and not greater than the allocated green time in the signal timing, i.e., $G_{(i,p)}(k) \in [0, u_{i,p}(k)]$. Other than the aforementioned parameters, the system also include the following parameters:

- $l_{(i,p)}$: the lost time (yellow and all red time),
- $r_{(j,q)_{(i,p)}}(k)$: the percentage of vehicles from VPL (j,q) that will flow into VPL (i,p) at time step k,
- $C(k)$: cycle length at time step k, and
- $In_{(i,p)}(k)$: flow demand of VPL (i,p) at time step k when the (i,p) is at the boundary of the network, i.e., $V_{(i,p)} = \varnothing$.

The number of vehicles on a VPL, $X_{(i,p)}(\cdot)$, is controlled by the fully used green time equivalents of downstream and upper stream intersections. From the physical road network view, the number of vehicles at one link is controlled by the intersections at both end of the link. For the case that the VPL is on the boundary of the network, the number of vehicles on that VPL is only control by the downstream intersection. This relationship can be express in Equation 3.

$$X_{(i,p)}(k+1) - X_{(i,p)}(k) = \begin{cases} \sum_{(j,q)\in V_{(i,p)}} \left(r_{(j,q)_{(i,p)}}(k) \times G_{(j,q)}(k) \times s_{j,q} \right) - G_{(i,p)}(k) \times s_{i,p}, & V_{(i,p)} \neq \varnothing \\ C(k) \times In_{(i,p)} - G_{(i,p)}(k) \times s_{i,p}(k), & V_{(i,p)} = \varnothing \end{cases} \quad \forall i,p,k \tag{3}$$

The allocated green times should follow the ring-and-barrier rules that are described in Equation 4,5, and 6.

$$\sum_{p\in P_{r_i,b}} \left(u_{i,p}(k) + l_{(i,p)}(k) \right) = \sum_{p\in P_{r_j,b}} \left(u_{i,p}(k) + l_{(i,p)}(k) \right) \quad \forall r_i, r_j \in \mathfrak{R}, b \in \mathfrak{B}, k \in \mathbb{N}_+ \tag{4}$$

$$\sum_{b\in\mathfrak{B}} \sum_{p\in P_{r_i,b}} \left(u_{i,p}(k) + l_{(l,p)}(k) \right) = C(k) \quad \forall r_i, r_j \in \mathfrak{R}, b \in \mathfrak{B}, k \in \mathbb{N}_+ \tag{5}$$

$$u_{i,p}^- \leq u_{i,p}(k) \leq u_{i,p}^+ \quad \forall i,p,k \tag{6}$$

Where:

$u_{i,p}^-$: the minimum green time for phase p at intersection i,

$u_{i,p}^+$: the green split minus the loss time of phase p at intersection i,

$\mathfrak{R}$: the set of rings in the ring-barrier controller,

$\mathfrak{B}$: the set of barrier sides in the ring-barrier controller, and
$P_{r,b}$: the set of phases in ring r, barrier side b.

The current VPL model does not address the scenario where the right turn movement does not move with the through movement. The studied area had multiple channelized right-turn lanes. Right turn movements at certain road links needed to be modeled separately from the through movement. We address this by separating the VPL, (i,p), for a through and right turn phase, p, into a through movement VPL, (i,p^T), and a right turn movement VPL, (i,p^R). Equation 3 still holds. The change is that p now could be from set $\{1,2,3,...,8,2^T,2^R,4^T,4^R,6^T,6^R,8^T,8^R\}$ when necessary. For the case where right turn movements that are not controlled, we can set the allocated green time to be equal to the cycle length, i.e., $G_{(i,p^R)} = C$. Overlap phases can be treated using the same philosophy.

It should be noted that a physical road link is not always viewed as two VPL (one for the left-turn phase and the other one for the through and right-turn phase). In the case of splitting phase control (e.g., the setting in the study site), a side street link is viewed as one VPL (representing the phase for that side street).

Solving optimal signal timing for an arterial via a top down approach

The VPL model was designed for Model Predictive Control (MPC) which is an online feedback control algorithm. In this work, the controllers did not have real-time control capabilities. We therefore downgrade the MPC algorithm to an offline timing optimization algorithm. We set the horizon to be a large number N (in this case, $N = 40$ cycles) and fixed the signal timing for the horizon ($u_{i,p}(\cdot) = \hat{u}_{i,p}$). We set the initial condition to be that each VPL has the number of vehicles that equals half of the space capacity of the VPL, i.e., $X_{i,p}(0) = \frac{c_{i,p}}{2}$. The optimization objective is to minimize and balance the number of vehicles across the network through the horizon as described in Equation 7. We used IPOPT (*15*) to solve the optimal signal timing.

$$\min J = \sum_{k=0}^{N} \sum_{\forall i,p} \left(\left(X_{(i,p)}(k+1) \right)^2 + \lambda \left(\hat{u}_{i,p} - G_{(i,p)}(k) \right)^2 \right) \tag{7}$$

We obtained the demand and turning rate data using video detection cameras installed along the corridor. We adopted the saturation flow rates that were calculated in Synchro traffic analysis software. The cycle length and lost times were given by Chattanooga Department of Transportation (DOT).

RESULTS AND DISCUSSIONS

We used Vissim to simulate the baseline scenario. We imported the road network and signal control timings from the Synchro file obtained from Chattanooga DOT. We obtained the vehicle volume and turning rate through APIs for the video detection system. The simulation period was one hour plus five minutes of warm-up time.

We collected eastbound and westbound travel times through the arterial and the number of vehicles passing the arterial. It should be noted that each intersection should have higher volume since many vehicles left the arterial before the end of it (e.g., through the ramps or to the mall). We used a node in Vissim to evaluate the energy consumption in the area. Figure 3 shows the evaluation node and travel time measures configurations.

We used the signal timing imported from the synchro file for the afternoon peak hours as the baseline setting. We simulated the optimized signal timing with the same demand as the baseline simulation. Compared with the baseline simulation, we found both travel time along the arterial

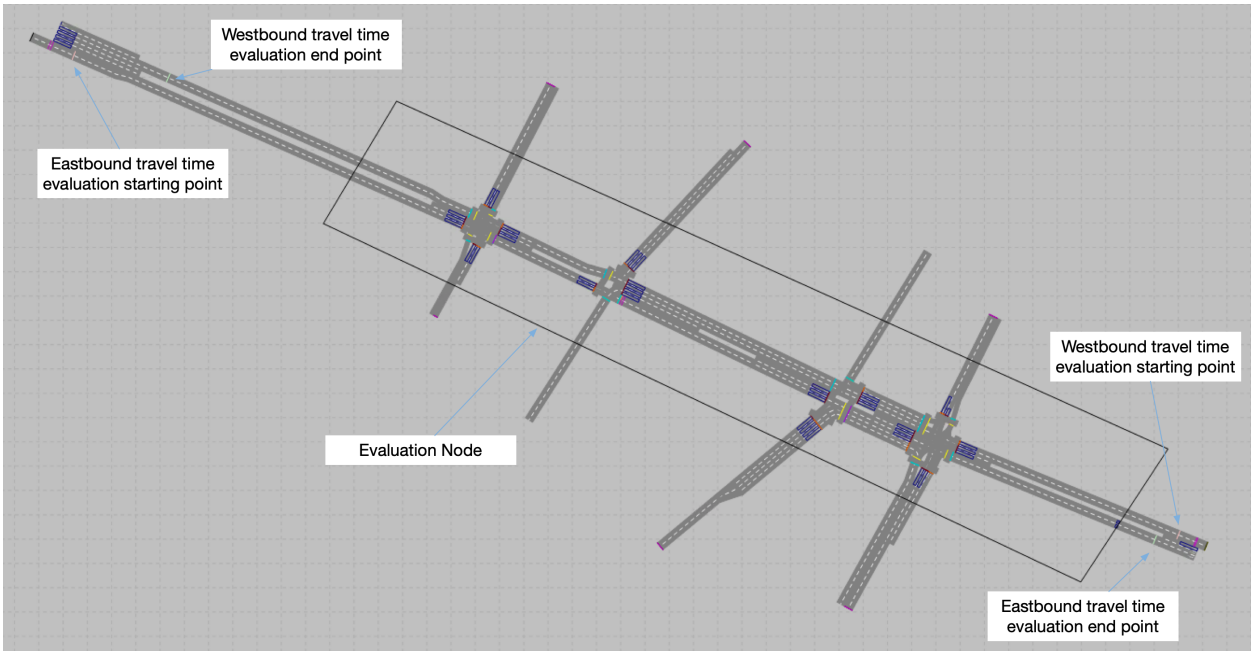

FIGURE 3 The evaluation node and travel time measures in Vissim

and the through put were improved. The eastbound travel time was reduced from 839 seconds to 281 seconds (66.5% reduction); the westbound travel time was reduced from 215 seconds to 141 seconds (34.4% reduction). The eastbound through put within the simulated hour was increased from 80 vehicles to 889 vehicles; and the westbound through put within the simulated hour was increased from 276 vehicles to 688 vehicles. The fuel consumption was reduced from 542 gallon to 452 gallon (16.6% reduction).

The simulation results showed that the optimized arterial signal timing using the proposed method performed better than the optimized signal timing using conventional bottom-up approach. The benefits came from two ways: 1) the proposed signal timing tend to hold excessive traffic in the longer links (in this case, before intersection A eastbound and before intersection D westbound); 2) the proposed signal timing provided better consistency in intersection capacities along the arterial which reduced the impact of the bottleneck intersections.

We presented the results to Chattanooga DOT. With minor tweaks in the timing, the engineers implemented the timing for the afternoon peak hours for week day. The local week day definition in the controllers is Monday through Thursday because Friday had much more traffic to the mall compared with the other week day. The initial implementations encountered some technical difficulties in setting the new timings. We eventually collected two-day data before the COVID-19 hit. One of the days had an accident in the nearby highway and significantly changed the traffic behavior.

We received positive feedback from the Chattanooga DOT for having a smoother traffic along the corridor. We collected sub-link level speed data through TomTom (a traffic data service) which utilized probe vehicles' data. We estimated the energy consumption via RouteE algorithm (*16*). We used TomTom speed, improved volume estimations from TomTom volume (*17*), grades information obtained from United States Geological Survey (USGS), and link length as inputs to get the estimations of Gasoline Gallon Equivalent (GGE). Figure 4 to 7 showed the estimated

averaged energy consumption per vehicle per mile. We weighted averaged the energy for the eastbound traffic and westbound traffic by volume. We also compared three different days' data each representing the standard control before implementing the new timing, the new signal timing from offline MPC algorithm that was proposed in this paper, and traffic under COVID-19 impact. Knowing that the effective experiment period was short and we could not get enough data to have statistically significant conclusion, we present these data here for qualitative presentation and exploring future work. We can see that we overall, although not significantly, reduced the energy usage along the arterial. Figures 8 and 9 show that, even under similar demand, we did significantly improved the eastbound speed at intersection B, which was an existing bottle neck, during the optimized time.

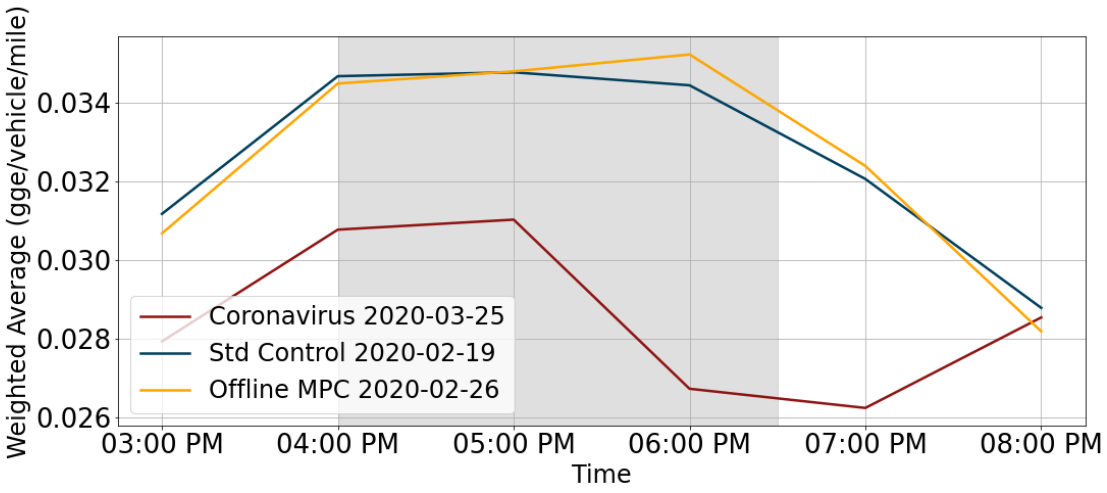

FIGURE 4 Energy consumption estimation for Shallowford Rd. at intersection A

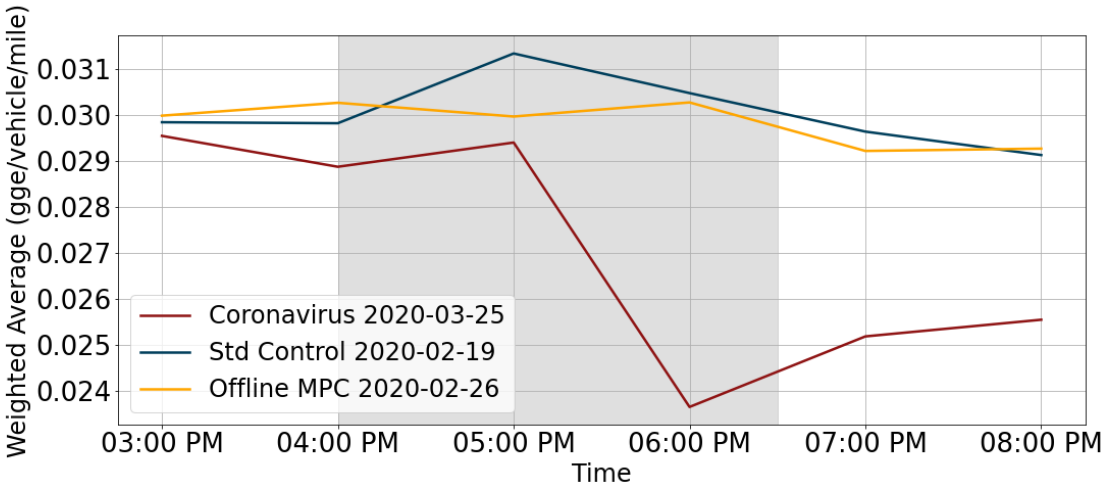

FIGURE 5 Energy consumption estimation for Shallowford Rd. at intersection B

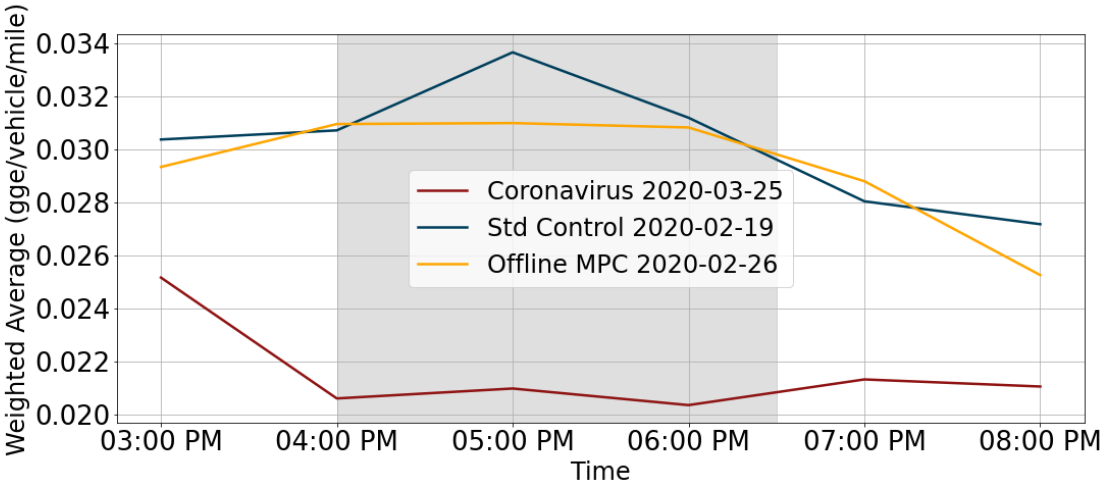

FIGURE 6 Energy consumption estimation for Shallowford Rd. at intersection C

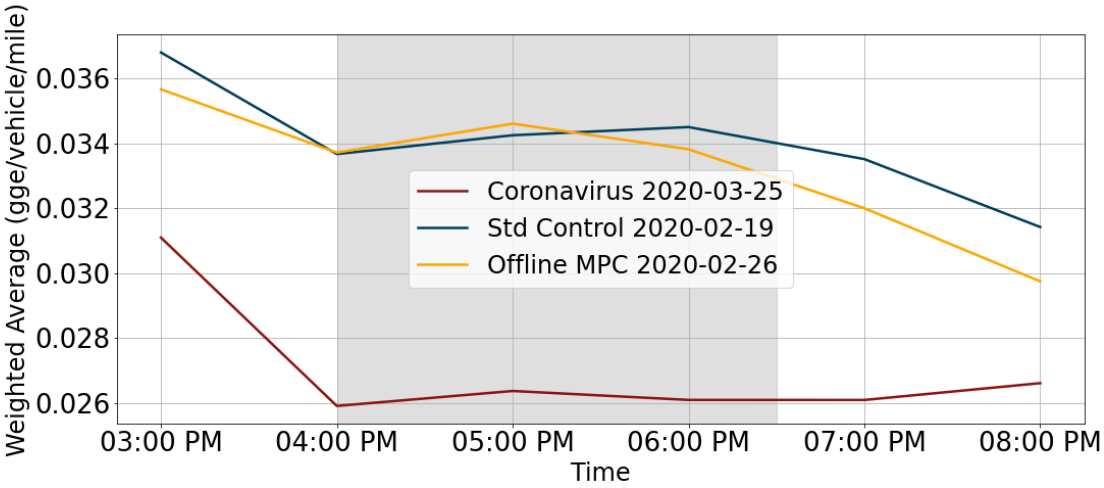

FIGURE 7 Energy consumption estimation for Shallowford Rd. at intersection D

Remaining Issues and Potential Solutions

Through this experiment, we found two remaining issues, i.e., 1) the demand measured by the video detection is not accurate; and 2) the downstream intersections of the controlled arterial suffered from higher volume from the controlled area.

The video detection at intersections can only see around the intersections. The volumes observed around the intersections are already impacted by the traffic signal control. When the traffic is over-saturated, the video detection at intersections can only measure the service rate, i.e., the volumes that the signal controls allowed to enter the intersections. One solution for that is to have advanced system detectors in the upstream portion of the links to detect the inflow. The detection at intersections can still provide good estimations of the turning rates. For the intersections without advanced system detectors, volume estimations from probe data can be used (*17*).

In the simulation, we didn't simulate the intersections that were not controlled. In the field

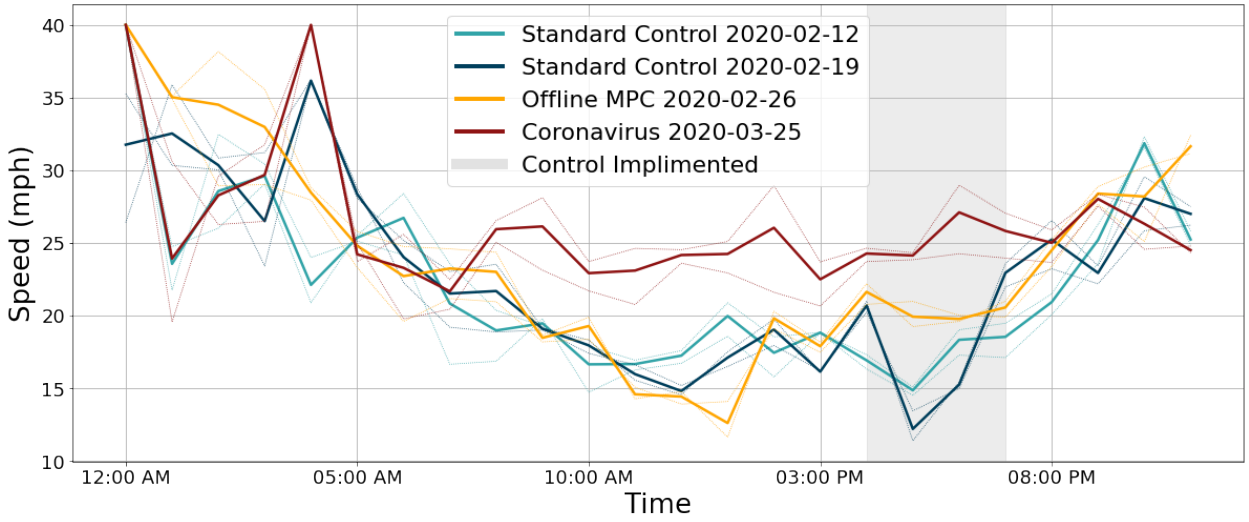

FIGURE 8 Eastbound speed for Shallowford Rd. at intersection B

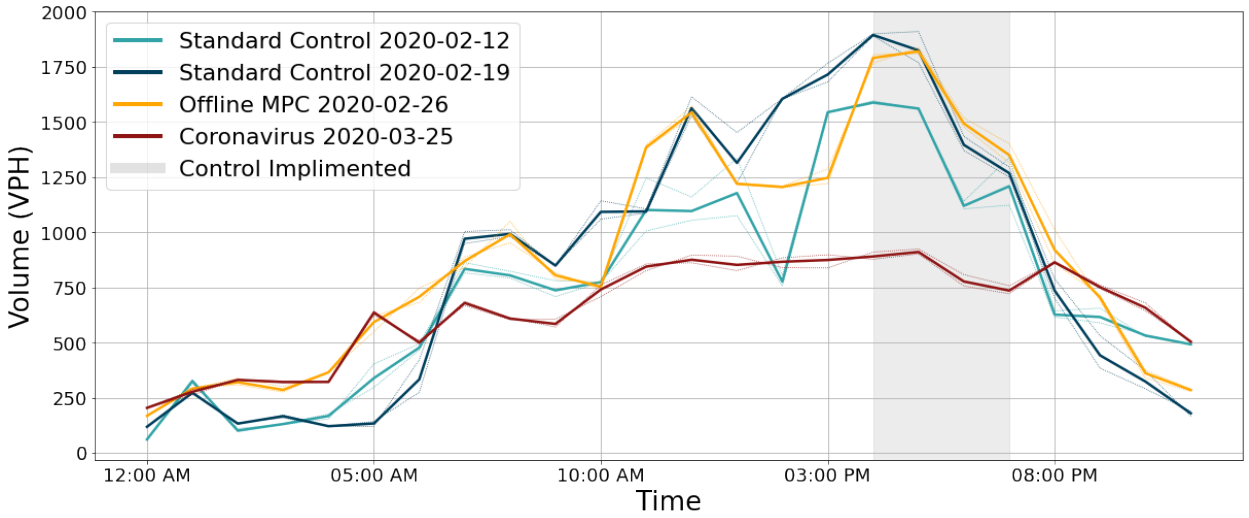

FIGURE 9 Eastbound volume for Shallowford Rd. at intersection B

implementation, we observed that the downstream intersections had queue spilled back. Although the queue spilled back in the controlled intersection from time to time, the controls managed to stabilize the queue within a few cycle. We believe that this was caused by the fluctuations in demand. However, the fact that we did not model the downstream intersections could cause the excessive flow for the downstream intersections. While we can always expand the boundary and include more intersections in the model, there will often be intersections that are outside of the controlled area (e.g., beyond jurisdictions). To minimize the negative impact on the downstream intersections, we could add downstream intersections' timing as constraints to the signal timing optimization problem. For a downstream VPL (i_d, p_d), we can obtain the existing allocated green time, $u^E_{i_d,p_d}$. With $G_{(i_d,p_d)}(k) \leq u^E_{i_d,p_d}$, the dynamics of the downstream VPL can be represented by

Equation 8.

$$X_{(i_d,p_d)}(k+1) - X_{(i_d,p_d)}(k) = \sum_{(j,q)\in V_{(i_d,p_d)}} \left(r_{(j,q)_{(i_d,p_d)}}(k) \times G_{(j,q)}(k) \times s_{j,q} \right) - G_{(i_d,p_d)}(k) \times s_{i_d,p_d} \quad \forall k \tag{8}$$

Adding the space capacity constraint to the downstream VPL, $X_{(i_d,p_d)}(k) \in [0, c_{i_d,p_d}]$, and adding VPL, (i_d, p_d), to the set of VPLs to be optimized in the objective function, we can regulate the output flow to the downstream intersection within a range that can be handled by the down stream intersections. The new objective function addressing the downstream intersections outside of the controlled network is:

$$\min J = \sum_{k=0}^{N} \sum_{\forall i,p} \left(\left(X_{(i,p)}(k+1) \right)^2 + \lambda \left(\hat{u}_{i,p} - G_{(i,p)}(k) \right)^2 \right) + \sum_{k=0}^{N} \sum_{\forall (i_d,p_d)} \left(X_{(i_d,p_d)}(k+1) \right)^2 \tag{9}$$

No new ring-barrier constraints are needed for the downstream intersections outside of the controlled network.

CONCLUSIONS AND FUTURE WORK

Certain assumptions in classical signal timing optimization procedures do not always hold when the intersections are closely spaced and the demand is high. It will be ideal if a control strategy can minimize the delay. However, the goal of signal control in the high demand and closely spaced intersection cases are usually to make the control "work", i.e., to move the traffic.

We found that a cause of arterial bottleneck is the inconsistency of intersections' capacities, which are impacted by the signal timings. An approach to make the control "work" is to ensure consistency among the arterial intersections' capacities. We also found that the VPL-based traffic signal MPC implies the consistency among intersections' capacities. The VPL-based model also exploits the room to allow queue spill back in links with larger space storage capacities.

We modified the VPL model to address the unique characteristics on the Shallowford Rd. corridor. We also downgrade the VPL-based MPC approach to an offline signal timing approach. We expanded the VPL model to address the real-world settings at Shallowford Rd. The simulation showed that the optimized signal timing can improve arterial throughput, reduce delay and reduce fuel consumption in the region significantly. A short field implementation also received positive feedback from Chattanooga DOT and a traveler who frequently used the studied area. We will collect more data when the traffic in the region get back to normal.

We are implementing the online version of the VPL-based MPC in the field in the summer of 2020 using real-time data feed.

ACKNOWLEDGEMENTS

This work was supported by the U.S. Department of Energy (U.S. DOE). The contents of this paper reflect the view of the authors who are responsible for the facts and accuracy of the data presented herein. The contents do not necessarily reflect the official view or policies of the U.S. DOE. This work was only made possible through the close cooperation of Chattanooga Department of Transportation. The research team acknowledges and appreciates particular guidance and technical support from Cindy Shell, Tommy Trotter, and Kevin Comstock.

AUTHOR CONTRIBUTIONS

The authors confirm contributions to the paper as follows: conception, program development, simulation, analysis, and draft manuscript preparation: Qichao Wang; data preparation and analysis: Joseph Severino and Juliette Ugirumurera; project management: Wesley Jones and Jibonananda Sanyal. All authors reviewed the results and approved the final version of the manuscript.

REFERENCES

1. Abbas, M., D. Bullock, and L. Head, Real-time offset transitioning algorithm for coordinating traffic signals. *Transportation Research Record*, Vol. 1748, No. 1, 2001, pp. 26–39.
2. Wang, Q. and M. Abbas, Visualizing vehicle arrivals in coordinated arterials using a colored PCD concept. In *2017 IEEE 20th International Conference on Intelligent Transportation Systems (ITSC)*, IEEE, 2017, pp. 1–6.
3. Wang, Q. and M. Abbas, Optimal Urban Traffic Model Predictive Control for NEMA Standards. *Transportation Research Record*, Vol. 2673, No. 7, 2019, pp. 413–424.
4. Wang, Q. and M. Abbas, Comparing and Contrasting NEMA-based Virtual Phase-Link control with Max Pressure Control in Arterial Signal Systems. In *2019 IEEE Intelligent Transportation Systems Conference (ITSC)*, 2019, pp. 1361–1366.
5. Abbas, M. M., Q. Wang, and C. C. McGhee, *From Functional Requirements to Validation: Development of a BADASS Simulation-Based Optimization of Preempted Signal Systems*, 2018.
6. Dabiri, S. and M. Abbas, Arterial traffic signal optimization using Particle Swarm Optimization in an integrated VISSIM-MATLAB simulation environment. In *2016 IEEE 19th International Conference on Intelligent Transportation Systems (ITSC)*, IEEE, 2016, pp. 766–771.
7. Hunt, P., D. Robertson, R. Bretherton, and R. Winton, *SCOOT-a traffic responsive method of coordinating signals*, 1981.
8. Lowrie, P., Scats, sydney co-ordinated adaptive traffic system: A traffic responsive method of controlling urban traffic, 1990.
9. Diakaki, C., M. Papageorgiou, and K. Aboudolas, A multivariable regulator approach to traffic-responsive network-wide signal control. *Control Engineering Practice*, Vol. 10, No. 2, 2002, pp. 183–195.
10. Yin, Y., Robust optimal traffic signal timing. *Transportation Research Part B: Methodological*, Vol. 42, No. 10, 2008, pp. 911–924.
11. TRB, *Highway Capacity Manual, Sixth Edition: A Guide for Multimodal Mobility Analysis*, Vol. 4. Transportation Research Board, 6th ed., 2016.
12. Liu, H., C. Claudel, R. Machemehl, and K. A. Perrine, A Robust Traffic Control Model Considering Uncertainties in Turning Ratios. *arXiv preprint arXiv:2002.06281*, 2020.
13. Jibonananda, S., *Real-Time Data and Simulation for Optimizing Regional Mobility in the United States*. `https://www.energy.gov/sites/prod/files/2020/06/f75/eems061_sanyal_2020_o_4.27.20_453PM_JL.pdf`, 2020.
14. Tian, Z., C. Messer, and K. Balke, Modeling Impact of Ramp Metering Queues on Diamond Interchange Operations. *Transportation Research Record*, Vol. 1867, No. 1, 2004, pp. 172–182.
15. Wächter, A. and L. T. Biegler, On the implementation of an interior-point filter line-search algorithm for large-scale nonlinear programming. *Mathematical programming*, Vol. 106, No. 1, 2006, pp. 25–57.
16. Holden, J., N. Reinicke, and J. Cappellucci, *RouteE: A Vehicle Energy Consumption Prediction Engine*. SAE Technical Paper, 2020.
17. Hou, Y., S. E. Young, A. Dimri, and N. Cohn, *Network Scale Ubiquitous Volume Estimation Using Tree-Based Ensemble Learning Methods*. National Renewable Energy Lab.(NREL), Golden, CO (United States), 2018.